



Targeting the initiation and termination codons of SARS-CoV-2 spike protein as possible therapy against COVID-19: the role of novel harpagide 5-O- β -D-glucopyranoside from *Clerodendrum volubile* P Beauv. (Labiatae)

Ochuko L. Erukainure^a , Olubunmi Atolani^b , Aliyu Muhammad^c , Sanusi B. Katsayal^c, Osadolor O. Ebhuoma^d, Collins U. Ibeji^e and M. Ahmed Mesaik^{f,g}

^aDepartment of Pharmacology, University of the Free State, Bloemfontein, South Africa; ^bDepartment of Chemistry, University of Ilorin, Ilorin, Nigeria; ^cDepartment of Biochemistry, Ahmadu Bello University, Zaria, Nigeria; ^dSchool of Agricultural, Earth and Environmental Sciences, University of KwaZulu-Natal, Durban, South Africa; ^eDepartment of Pure and Industrial Chemistry, University of Nigeria, Nsukka, Nigeria; ^fDr. Panjwani Center for Molecular Medicine and Drug Research, International Center for Chemical and Biological Sciences, University of Karachi, Karachi, Pakistan; ^gFaculty of Medicine, University of Tabuk, Tabuk, Kingdom of Saudi Arabia

Communicated by Ramaswamy H. Sarma

ABSTRACT

The global spread of the coronavirus infections disease – 2019 (COVID-19) and the search for new drugs from natural products particularly from plants are receiving much attention recently. In this study, the therapeutic potential of a new iridoid glycoside isolated from the leaves of *Clerodendrum volubile* against COVID-19 was investigated. Harpagide 5-O- β -D-glucopyranoside (HG) was isolated, characterised and investigated for its druglikeness, optimized geometry, and pharmacokinetics properties. Its immunomodulatory was determined by chemiluminescence assay using polymorphonuclear neutrophils (PMNs) in addition to T-cell proliferation assay. *In silico* analysis was used in determining its molecular interaction with severe acute respiratory syndrome coronavirus-2 (SARS-CoV-2). HG displayed potent druglikeness properties, with no inhibitory effect on cytochrome P₄₅₀ (1A2, 2C19, 2C9, 2D6 and 3A4) and a predicted LD₅₀ of 2000 mg/kg. Its ¹H-NMR chemical shifts showed a little deviation of 0.01 and 0.11 ppm for H-4 and H-9, respectively. HG significantly suppressed oxidative bursts in PMNs, while concomitantly inhibiting T-cell proliferation. It also displayed a very strong binding affinity with the translation initiation and termination sequence sites of spike (S) protein mRNA of SARS-CoV-2, its gene product, and host ACE2 receptor. These results suggest the immunomodulatory properties and anti-SARS-CoV-2 potentials of HG which can be explored in the treatment and management of COVID-19.

ARTICLE HISTORY

Received 11 May 2020
Accepted 18 October 2020

KEYWORDS


Clerodendrum volubile;
COVID-19; harpagide 5-O- β -D-glucopyranoside; SARS-CoV-2; and spike protein

Introduction

The recent pandemic of coronavirus disease 2019 (COVID-19) has led to an unprecedented rate of mortality, with Italy, China, Spain and USA being the most hit (WHO., 2020). It is caused by the novel β -coronavirus (enveloped non-segmented positive-sense RNA virus), SARS-CoV-2 which has a similar sequence identity to that of bat/human severe acute respiratory syndrome coronavirus-related coronavirus (SARSr-CoV) and bat SARS-like coronavirus (SLCoV) (Guo et al., 2020; Schoeman & Fielding, 2019; Tian et al., 2020). Since its origin in Wuhan, China as a cluster of pneumonia cases in December 2019 which has spread globally (da Silva et al., 2020), there have been search for effective antiviral remedies against the diseases. Lack of effective treatment coupled with no valid vaccines increases the number of infections and mortalities on a daily basis (Mehta et al., 2020; Onder et al., 2020). The common symptoms of COVID-19 include sore throat, cough, fatigue, slight dyspnoea, headache, conjunctivitis, diarrhea and fever (Pascarella et al., 2020). The

major cause of COVID-19 mortality is respiratory failure as present treatments are based on symptomatic management and respiratory sustenance (Pascarella et al., 2020). Underlying ailments particularly diabetes mellitus and obesity have been implicated as high-risk factors of COVID-19 mortalities (Holman et al., 2020). Boosting the immune system has also been reported as a preventive strategy against COVID-19, as cytokine release syndrome (CRS) characterized by exacerbated levels of macrophage inflammatory protein 1- α , tumour necrosis factor- α (TNF- α), interleukins (IL)-2 and -7, monocyte chemoattractant protein 1, and granulocyte-colony stimulating factor have been implicated in patients with severe conditions (Mehta et al., 2020; Shi et al., 2020). *In vitro* studies have reported the inhibitory effect of remdesivir and chloroquine on SARS-CoV-2 activity (Wang et al., 2020), and have shown some therapeutic effects in clinical trials (Wang et al., 2020). However, studies have reported deaths in COVID-19 patients treated with chloroquine and its derivatives owing to severe arrhythmias (Tang et al., 2020). It has

CONTACT Ochuko L. Erukainure  loreks@yahoo.co.uk; ErukainureOL@ufs.ac.za  Department of Pharmacology, University of the Free State, Bloemfontein 9300, South Africa

 Supplemental data for this article can be accessed online at <https://doi.org/10.1080/07391102.2020.1840439>.

© 2020 Informa UK Limited, trading as Taylor & Francis Group

also been shown to suppress the immune system as well as inhibit autophagy and xenophagy (Tang et al., 2020). Interestingly, the dynamics of the said virus largely depends on the molecular interactions between spike protein and human angiotensin converting enzyme 2 receptor (ACE2). Thus by implication, targeting these biomarkers have been reported as viable strategies for treating the disease (Gurwitz, 2020; Jiang et al., 2012).

The antiviral and immunomodulatory activities of medicinal plants have been reported (Erukainure, Mesaik, et al., 2017; Vijayan et al., 2004). This has been attributed to their ability to modulate inflammatory cytokines and phagocytic activities of monocytes, neutrophils and macrophages (Erukainure, Mesaik, et al., 2017; Harun et al., 2015), with their phytochemical constituents playing an influential role. *Clerodendrum volubile* is among medicinal plants reported for their immunomodulatory activities (Erukainure, Hafizur, et al., 2017; Erukainure, Zaruwa, et al., 2017; Erukainure et al., 2016).

Clerodendrum volubile is a leafy vegetable mostly utilized as food ingredients in Southern Nigeria (Erukainure, Sanni, et al., 2018; Erukainure et al., 2011). Regarded as magic leaves, *C. volubile* is used in folk medicine for treating ulcers, arthritis, rheumatism, dropsy, and diabetes (Burkill, 1985). Its antioxidant activities have been reported in diabetic rats, and cancerous cells which correlates with their antidiabetic and anticancer activities (Erukainure, Ashraf, et al., 2018; Erukainure, Hafizur, et al., 2017; 2018). The flowers as well as protocatechuic acid and pectolinarigenin isolated from the leaves have been reported for their ability to modulate phagocytic oxidative burst in isolated neutrophils and macrophages which demonstrates their immunomodulatory activities (Erukainure, Hafizur, et al., 2017; Erukainure, Mesaik, et al., 2017; Erukainure et al., 2016). The dichloromethane (DCM) fraction of the leaves have been reported for its cytotoxic effect on human embryonic kidney (HEK293) cells (Erukainure, Narainpersad, et al., 2018). The leaves are rich in phenolics contents which has been correlated with its reported biological activities (Erukainure, Narainpersad, et al., 2018; Oboh et al., 2017).

To the best of our knowledge, this study reports for the isolation and characterization of a new iridoid glycoside, harpagide 5-O- β -D-glucopyranoside from the leaves of *C. volubile*. Based on previous reports on the immunomodulatory properties of the leaf extract, it is hypothesized that the isolated compound may contribute to the modulation of the immune system in favor of suppressing CRS. Thus, this study was aimed at investigating the antioxidative burst potentials of the compound on polymorpho-nuclear neutrophils (PMNs), as well as its antiproliferative effect on T-cells. The ability of the compound to suppress the activity of SARS-CoV-2 was investigated using combined *in silico* tools. This study also reports global epidemiology study of COVID-19 from January – August 2020.

Materials and methods

Instrumentation

The ^1H - and ^{13}C -NMR spectra were recorded at temperature 300 K on Bruker Avance 500 MHz spectrometer in MeOD. δ

(ppm) values were used for reporting chemical shifts. The ^1H -NMR spectrum was recorded for 128 scan using pulse sequence with an acquisition time 1.58 sec, relaxation delay of 1.5 sec, spectra width of 10,330 Hz and Intrinsic digital resolution of 0.3152 Hz with tetramethylsilane, TMS as internal standard. Hitachi UV-3200 spectrophotometer was used in obtaining UV spectra. A pre-coated silica gel 60 F₂₅₄ plates (E. Merck, 0.25 mm) was used for thin layer chromatography (TLC), which was detected under UV light (254 nm) after spraying with ceric sulphate reagent. JEOL JMS-HX-110 mass spectrometer was used for recording EI-MS.

Softwares

Computational software used for this work includes ArcGIS 10.6 software, UCSF Chimera (v. 1.0.1), Discovery Studio 2017 R2 Client (v17.2.0.16349), Python prescription virtual screening software (PyRx, 8.0), ChemDraw Ultra v12.0.2, PatchDock server and other online computational tools available.

Global modelling and spatial mapping of COVID-19

We obtained freely available daily data of confirmed cases and deaths for Coronavirus Disease (COVID-19) pandemic across the world from the COVID-19 – Statistics and Research website from January 2020 to March 2020 (Roser et al., 2020; ECDC, 2020). The COVID-19 – Statistics and Research team retrieves daily global and national statistics of COVID-19 from two credible sources, the World Health Organization (WHO) and, the European Centre for Disease Prevention and Control (ECDC). We aggregated the daily confirmed data (cases and deaths) for each country into monthly data for January to March 2020, and subsequently performed the spatiotemporal distribution analysis of COVID-19 confirmed cases and deaths using the ArcGIS 10.6 software (ESRI, Redland, CA, USA).

Plant material

Clerodendrum volubile leaves were obtained from local farmers at Ifon, Ondo State, Nigeria. The leaves were assigned a voucher number, UBHC₂₈₄ after identification and authentication by Dr. Henry Akinbosun at the Herbarium, Department of Botany, University of Benin, Benin City, Nigeria. The leaves were air-dried to minimize loss of volatiles and light-sensitive compounds (Thamkaew et al., 2020) before blending to fine powder and stored in a zip-lock bag at room temperature until further analysis (2 days).

Extraction and isolation

The blended sample was subjected to methanol (MeOH) extraction at room temperature. The solvent choice was based on the polarity of MeOH and reports as an optimal solvent for high content of phytochemical constituents (Truong et al., 2019). The extract was concentrated *in vacuo* using a rotary evaporator. About 100 g of the extract was dissolved in MeOH/Distilled water (1:3), and thereafter subjected to gradient polarity based chemical fractionation using, n-

hexane (Hex), n-dichloromethane (DCM), ethyl acetate (EtOAc), and butanol (BuOH). All the fractions were collected, concentrated *in vacuo* and stored in glass vials at -20°C . The EtOAc fraction was parked into a silica gel – loaded column chromatography for further fractionation. The column was subjected to solvent elution starting with 100% hexane, and thereafter mixtures of Hex and EtOAc (9:1) in increasing order of polarity up to 100% EtOAc. Each elute was collected in glass vials and its purity was confirmed by subjection to thin-layer chromatography on pre-coated silica gel 60 F₂₅₄ sheets. They were sprayed with ceric sulfate reagent, dried under hot-air (60°C), and viewed under UV light (254 nm). Elutes from Hex and EtOAc (8:2) showed a single spot. They were combined and concentrated in a fume compound, before subjection to NMR analysis for structural elucidation and identification. The compound was identified as harpagide 5-O- β -D-glucopyranoside.

Density functional theory (DFT) analysis

The isolated compound (harpagide 5-O- β -D-glucopyranoside) was fully optimized using density functional theory (DFT) with M06-2X functional with 6-31+G(d,p) basis. The frequency calculation was computed confirming no negative frequencies. The scaling factor of 0.964 was applied to evaluate vibrational frequencies (Johnson III, 1999). The ^1H magnetic shielding constants, by chemical shifts, obtained on a δ -scale relative to the TMS, used as reference was calculated on complex 1 and 2 using the Gauge-Independent Atomic Orbital (GIAO) method developed by Wolinski et al. (1990). Polarizable Continuum Model (PCM) through a single point (B3LYP/6-311+G(2d,p)) calculation was used for determining the ^1H NMR chemical shift (DMSO solvent: dielectric constant, $\epsilon = 46.826$) (Cances et al., 1997; De Souza et al., 2017).

Druglikeness analysis

To determine the druglikeness properties of the selected compounds, a supercomputing facility for Bioinformatics and Computational Biology (SCFBio platform; scfbio-iitd.res.in) was used. 3D structures of the compounds were submitted through the platform and the prediction carried out based on Lipinski's rule. Lipinski's rule considered five basic properties including molecular weight, hydrogen bond acceptor and donor, lipophilicity index (LogP) and molar refractivity of a compound (Jayaram et al., 2012; Lipinski, 2004).

Pharmacokinetics and lethal dose prediction

The pharmacokinetics and oral lethal dose of the isolated compound was determined *in silico* via qualitative structure activity relationship (QSAR) vis-à-vis virtual molecular structure activity relationship studies (SARs) using the SwissADME (Daina et al., 2017) and ProTox-II (Banerjee et al., 2018) respective online servers.

Luminol-amplified chemiluminescence assay

Blood sample was collected from a consented apparently healthy volunteer, from which neutrophils were immediately isolated as previously described (Alyiu et al., 2014). The isolated neutrophils were subjected to luminol-amplified chemiluminescence assay (Helfand et al., 1982). Briefly, the isolated neutrophils ($1 \times 10^6/\text{mL}$) were suspended in modified Hank's solution (MHS) and incubated with different concentrations (0.5, 5.00 and 50.00 $\mu\text{g}/\text{mL}$) of the isolated compound (harpagide 5-O- β -D-glucopyranoside) for 30 min. Zymosan (1 mg/mL) was thereafter added, followed by 25 μL of luminol (10^{-5} M). A luminometer (Lab system Luminoskan RS, Helsinki, Finland) was used in recording the total chemiluminescence (CL). Control (+C) consisted of MHS containing cells only.

T-cell proliferation assay

Blood obtained from a consented apparently healthy volunteer was subjected to Ficoll-Hypaque gradient centrifugation and proliferation to extract T-cells as described previously (Nielsen et al., 2003). The cells were cultured in a 96-well round bottom tissue culture plate at a concentration of $5 \times 10^5/\text{mL}$. They were thereafter stimulated with 1.25 mg/mL of phytohaemagglutinin and incubated with the isolated compound (0.5, 5.00 and 50.00 $\mu\text{g}/\text{mL}$) at 37°C in a 5% CO_2 incubator for 72 h. After incubation, the reaction was pulsed with titrated thymidine 0.5 $\mu\text{Ci}/\text{well}$, and further incubated for 18 h. The cells were harvested with a cell harvester (SKATRON A.S. Flow Lab., Norway) into a glass fibre-filter (Cambridge Technology USA), and measured by counting with a liquid scintillation counter. After 120 s, the counts per minute (cpm) results were recorded (Erukainure, Mesaik, et al., 2017). All studies were carried out under the ethical guidelines of the International Center for Chemical and Biological Sciences, University of Karachi, Karachi, Pakistan.

Molecular docking studies

SARS-CoV-2 spike protein mRNA sequence

SARS-CoV-2 spike protein mRNA sequence was obtained from the PubMed database from the coronavirus whole genome (NC_045512.2). About 42 nucleotide sequence from both initiation and termination codons (Table 1) were converted into 3D single mRNA strand and prepared for docking.

Molecular docking

The binding potentials of Harpagide 5-O- β -D-glucopyranoside, Azithromycin, Chloroquine, and Remdesivir was studied by means of molecular docking. The 3D crystal structures of 2019-nCoV spike protein receptor-binding domain bound with ACE2 angiotensin converting enzyme 2 receptor (ACE2) were downloaded from the protein data bank (PDB) with PDB ID; 6M0J (Lan et al., 2020) with resolution 2.45 Å. The suitable grid box was determined using AutoDock tools 1.5.4 (Sanner, 1999). The ligands (CID_2719, 121304016 and

Table 1. Selected sequence of initiation and termination sites of COVID-19 spike protein mRNA.

Sequence site	mRNA Sequence
Translation initiation site	5'-AUGUUUUUUUUUCUUGUUUUUUUUGCCACUAGUCUCUAGUCAG-3'
Translation termination site	5'-UCUGAGCCAGUGCUCUAAAGGAGUCAAAUUACAUUACACAUAA-3'

DB00207) were obtained from PUBMED, while the isolated compound (harpagide 5-O- β -D-glucopyranoside) was drawn using ChemDraw Ultra v12.0.2 and the file converted to pdb format. Initial optimization was done using Gaussian 09 (Frisch et al., 2009), to obtain minimized conformations. The determined dimension was $X=26$ $Y=26$ $Z=26$ with 1.00 Å as the grid spacing. The optimum binding site for the ligand (Erukainure et al., 2020; Yang et al., 2013) was determined using Lamarckian genetic algorithm method. Gasteiger charges were computed using the AutoDock Tools graphical user interface supplied by MGL Tools (Morris et al., 2009).

Statistical analysis

To address biological variability, wet experiments were repeated at least thrice. Where appropriate, results were presented as mean \pm SD and subjected to one-way analysis of variance (ANOVA). Tukey's HSD-multiple range post-hoc test was used in obtaining significant differences between means at $p < 0.05$. IBM Statistical Package for the Social Sciences (SPSS) for Windows, version 23.0 (IBM Corp., Armonk, NY, USA) was used for the analyses.

Results

Spatiotemporal distribution

The spatiotemporal distribution of confirmed monthly COVID-19 cases and deaths from January to March 2020 is shown in Figure 1. The maps suggest the impacts of the disease (cases and deaths) were initially felt in China in January 2020 before it spread to other countries where noticeable spikes in confirmed COVID-19 cases and deaths were reported in subsequent months. This suggests the epicentre of COVID-19 shifted from China to Europe (affecting mainly Italy, Spain, Germany, France, UK, Switzerland, Belgium, Netherlands, Turkey and Austria) at the end of March 2020. Other countries that reported high confirmed cases and deaths of COVID-19 in March 2020 were the USA, Iran, Canada, South Korea, Brazil and Chile. However, African countries reported fewer cases and deaths of COVID-19 compared to countries in other continents from January to March 2020. While low confirmed cases and deaths of COVID-19 are continuously reported across Africa, US and Europe (especially Spain, France and UK) are still characterized by high confirmed COVID-19 cases and death. Other countries currently experiencing a surge in COVID-19 cases and deaths are Russia, India, Indonesia, Philippines, Iran, Iraq and most South American Countries (especially Brazil, Columbia, Argentina, Peru, Mexico, Chile). This suggests, South America is currently the new epicentre of COVID-19 (Roser et al., 2020; ECDC, 2020).

Isolation of harpagide 5-O- β -D-Glucopyranoside

As shown in Figure 2, harpagide 5-O- β -D-glucopyranoside was isolated for the first time from the leaves of *C. volubile*. Its structure was elucidated using the combination of NMR, infrared and mass spectra data:

Harpagide 5-O- β -D-Glucopyranoside ($C_{12}H_{34}O_{15}$; Figure S1): IR (KBr) V_{max} : 3375 (OH), 2922, 2852 (C-H Str), 1461 (C=C, 1040 (C-O) cm^{-1} ; 1H NMR (500 MHz, CD_3OD) δ : 7.90 (1H, *d*, H-3), 5.80 (1H, *d*, H-1), 4.85 (1H, *d*, $J=5.0$ Hz, H-4), 4.90 (1H, *t*, H-6), 1.90 (2H, *dd*, H-7), 2.30 (1H, *d*, H-9), 4.55 (1H, *d*, H-1'), 3.90 (1H, *m*, H-6''a), 3.75-3.60 (4H, *m*, H-6'b, H-6''b, H-3', H-3''), 3.45-3.30 (4H, *m*, H-4', H-4'', H-5', H-5''), 3.25-3.16 (2H, *dd*, $J=1.5, 1.5$ Hz, H-2'; H-2''), 3.95 (2H, *m*, H-6'a, H-6''a). EI-MS: m/z 368 FAB-MS: m/z 549 calculated for $[M + Na]^+$, that is $C_{12}H_{34}O_{15}Na$. Fragment of de-glucosidated at m/z 387.21 corresponds to $[M - Gluc + 2H]^+$ calculated for $C_{15}H_{24}O_{10}$.

Harpagide 5-O- β -D-glucopyranoside:

DFT analysis

The optimized geometry of harpagide 5-O- β -D-glucopyranoside with the key interatomic distances in Angstrom are shown in Figure 3. The calculated broad peak at 3401 cm^{-1} is assigned to the O—H of the cyclopentane ring. The aromatic ring C=C and C—H stretching vibrations are assigned 1471 and 2851 cm^{-1} respectively. The C—O—C stretching vibrations are assigned the strong peaks at 1090. The calculated 1H -NMR spectrum for harpagide 5-O- β -D-glucopyranoside is presented in Table 2. Major hydrogen atoms are designated in the calculated 1H -NMR spectrum.

Druglikeness analysis

Drug likeness properties of the selected compounds were determined using criteria put forward by Lipinski. The result present in Table 3 and presents shown shows the parameter assessed, the scores and the reference value for each parameter, respectively. Harpagide 5-O- β -D-glucopyranoside showed strong compliance with respect to number of hydrogen bond donors, LogP and molar refractivity, except for hydrogen bond acceptors.

Pharmacokinetics and lethal dose prediction

In silico prediction analysis predicted harpagide 5-O- β -D-glucopyranoside to be absorbed poorly in the gastrointestinal tract and not permeable across the blood brain barrier (BBB) as shown in Table 4. Harpagide 5-O- β -D-glucopyranoside was also predicted as a P-glycoprotein inhibitor. The compound was predicted not to be an inhibitor of cytochromes

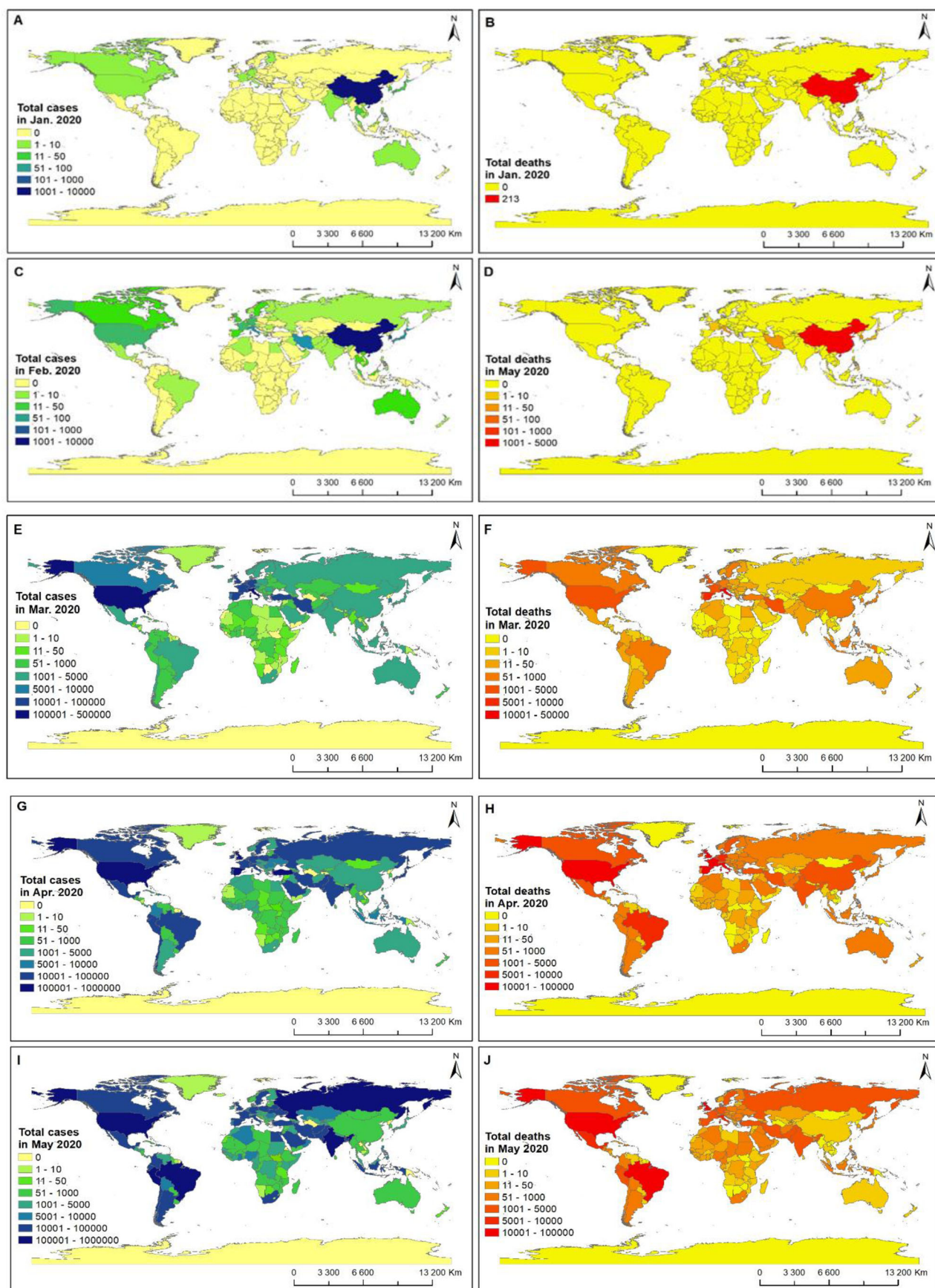


Figure 1. Total monthly confirmed cases and deaths of COVID-19, January 2020–August 2020. Source: ECDC, 2020; Roser et al., 2020. **Key:** A = total confirmed cases in January; B = total deaths in January; C = total confirmed cases in February; D = total deaths in February; E = total confirmed cases in March; F = total deaths in March; G = total confirmed cases in April; H = total deaths in April; I = total confirmed cases in May; J = total deaths in May; K = total confirmed cases in June; L = total deaths in June; M = total confirmed cases in July; N = total deaths in July; O = total confirmed cases in August; and P = total death in August. Jan. = January, Feb. = February, Mar. = March, Apr. = April, Jun. = June, Jul. = July, and Aug. = August.

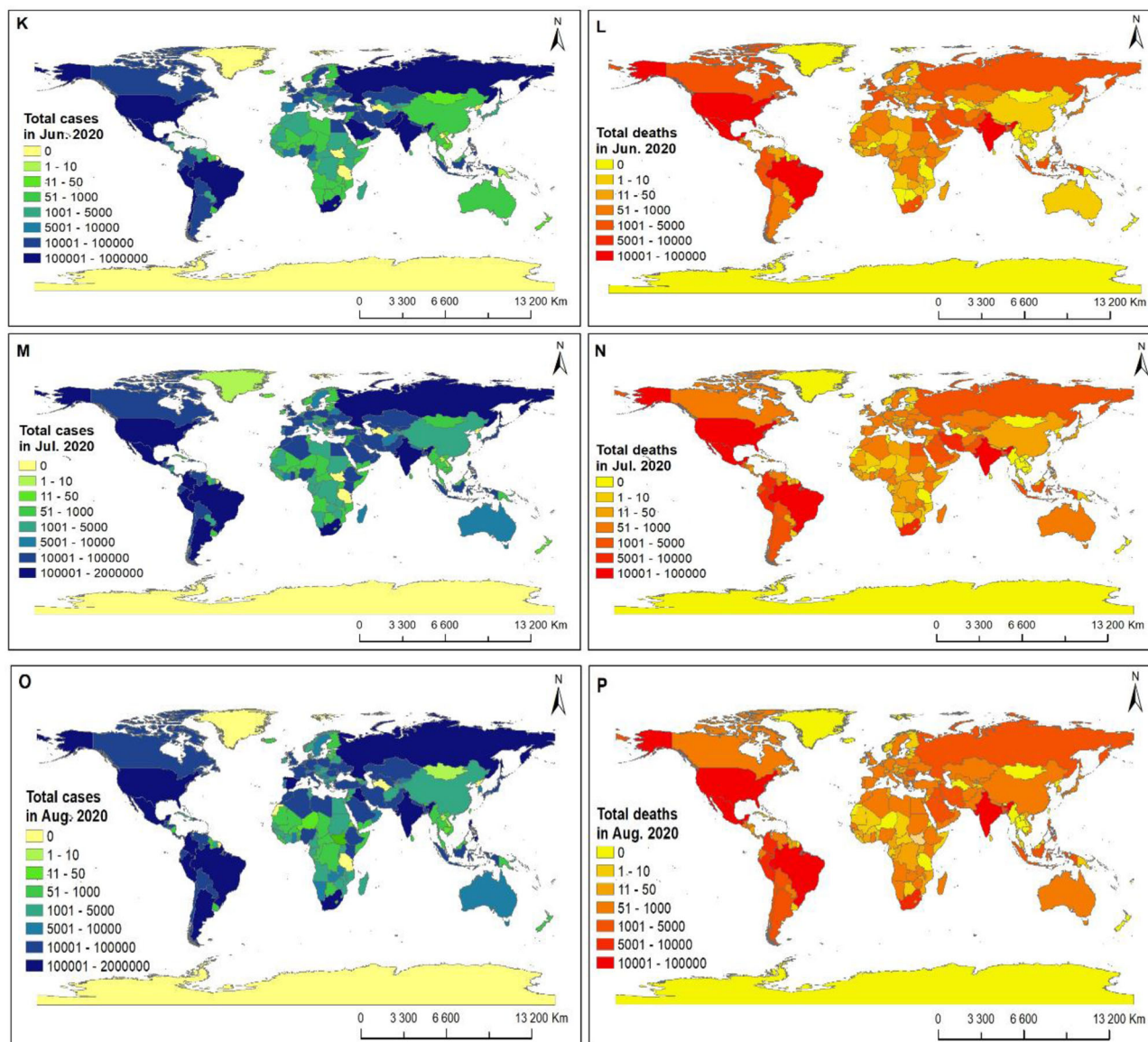


Figure 1. Continued

P450 (CYPs) 1A2, 2C19, 2C9, 2D6 and 3A4. The oral LD_{50} was predicted to be 2000 mg/kg, with a toxicity class of 4.

Effects on respiratory oxidative burst and T-cell proliferation

As depicted in Figure 4A, incubation of harpagide 5-O- β -D-glucopyranoside with neutrophils significantly ($p < 0.05$) inhibited ROS production stimulated by zymosan in PMNs with an IC_{50} value of $0.33 \pm 0.01 \mu\text{g/mL}$. The activity was dose dependent with increasing concentration. The compound also significantly ($p < 0.05$) suppressed the proliferation of T-cell proliferation, with a 26% inhibitory activity compared to the control as shown in Figure 4B.

Molecular docking studies

The binding potentials of Harpagide 5-O- β -D-glucopyranoside and standard FDA approved drugs (Azithromycin,

Chloroquine, and Remdesivir) were studied by means of molecular docking. Ligand-protein interactions between viral protein (SARS-CoV-2 spike protein), the host receptor target (ACE2) and Harpagide 5-O- β -D-glucopyranoside are presented in Figures 5–7. Harpagide 5-O- β -D-glucopyranoside displayed a good binding in complex with the host receptor target, initiation and termination sequence of the viral spike protein messenger RNA compared to all studied standard drugs with binding affinities of -7.5 , -6.4 and $6.3 \text{ kcal mol}^{-1}$ respectively (Table 5). Interestingly, it showed comparable binding affinity with Remdesivir, when in complex with the SARS-CoV-2 spike protein with a slight difference of $0.2 \text{ kcal mol}^{-1}$ but better binding compared to Azithromycin and Chloroquine (Figures S2 and S3; and Table 5).

Discussion

As COVID-19 pandemic feasts, scientists and policy makers are currently making tireless efforts to reduce transmission

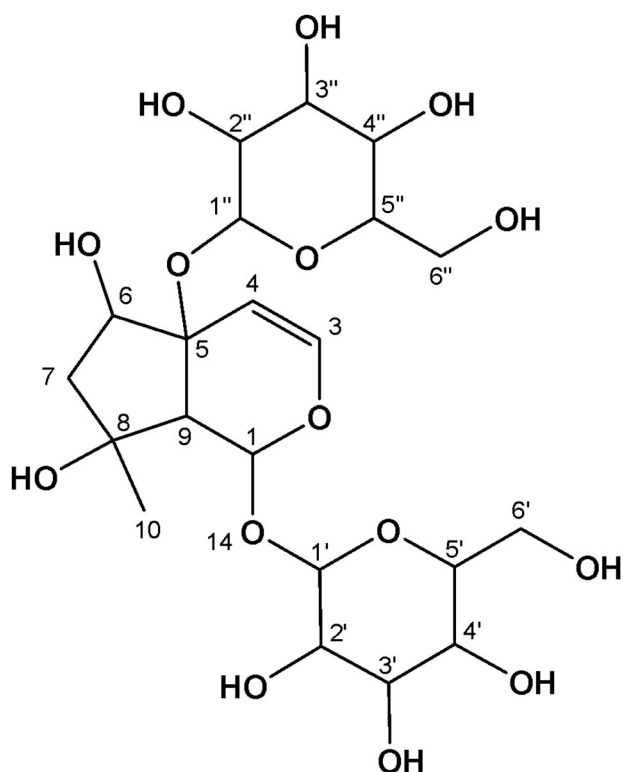


Figure 2. Harpagide 5-O- β -D-glucopyranoside was isolated from *C. volubile* leaves.

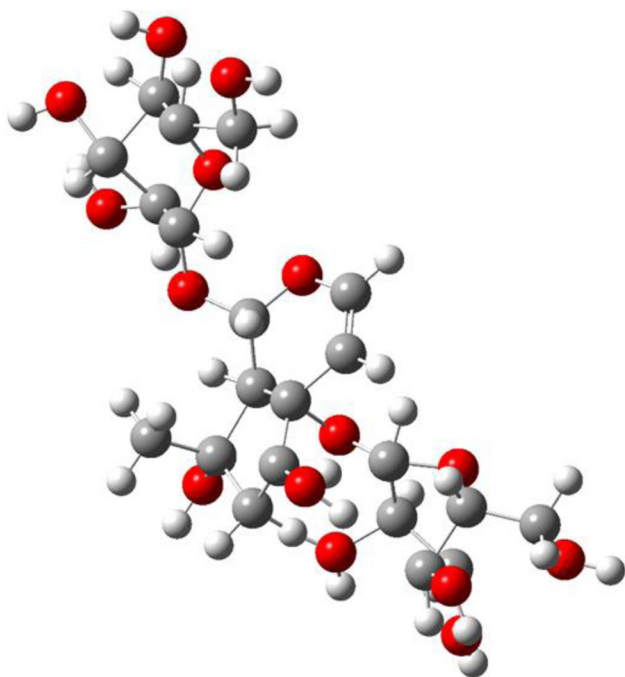


Figure 3. Optimized geometry of harpagide 5-O- β -D-glucopyranoside using density functional theory (DFT) with M06-2X functional with 6-31 + G(d,p) basis.

through regular public health interventions based on testing, isolation of cases and tracing of contacts (Mitjà & Clotet, 2020). Efforts are also on top gear in the area of vaccines development and clinical trial of drugs based on the general principles of drug repurposing (Zhou et al., 2020). Unfortunately, the search for new drugs using bioactive

Table 2. Selected experimental and theoretical ^1H chemical shift values (with respect to TMS, all values in ppm) for the compound.

Atoms	Experimental Chemical shift (ppm)	Calculated B3LYP/6-311 + G(2,d,p) Chemical shift (ppm)
H-1	5.80	6.10
H-3	7.90	6.55
H-4	4.85	4.86
H-6	4.90	5.14
H-9	2.30	2.41

Table 3. Drug like-predicted values based on lipinski's rule of five.

Parameters	Reference value	Harpagide 5-O- β -D-glucopyranoside
Molecular Weight	<500D	492
Hydrogen Bond Donors	<5	0
Hydrogen Bond Acceptors	<10	15
LogP	<5	-3.6
Molar Refractivity	40-130	94.6

Table 4. *In silico* predicted pharmacokinetics and LD50 values of harpagide 5-O- β -D-glucopyranoside.

Parameters	<i>In Silico</i> Prediction
GI absorption	Low
BBB permeant	No
P-gp substrate	Yes
CYP1A2 inhibitor	No
CYP2C19 inhibitor	No
CYP2C9 inhibitor	No
CYP2D6 inhibitor	No
CYP3A4 inhibitor	No
LD ₅₀	2000 mg/kg
Toxicity class	4

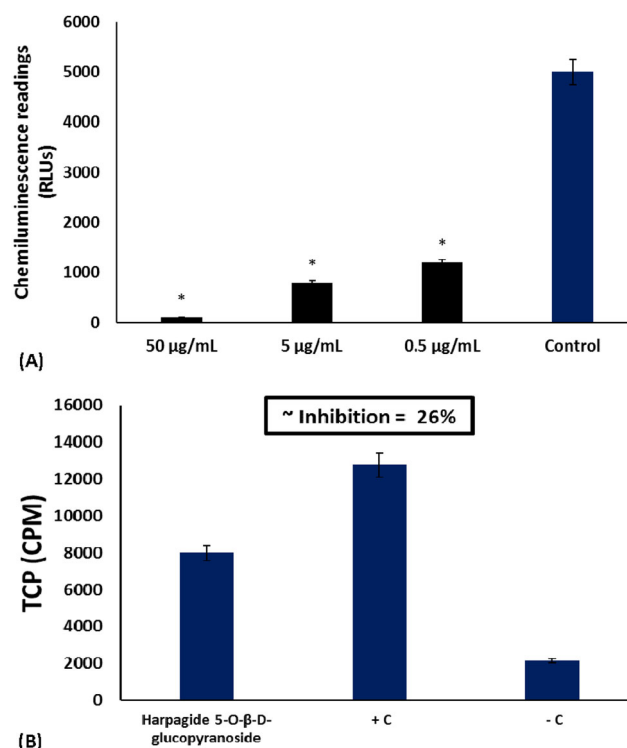


Figure 4. Effect of harpagide 5-O- β -D-glucopyranoside on (A) oxidative burst of neutrophils; and (B) T-cell proliferation. Values = mean \pm SD; $n=3$. + C = positive control; - C = negative control; RLUs = relative light units; TCP = T-cell proliferation; CPM = counts per minute. *Statistically significant ($p < 0.05$) compared to control.

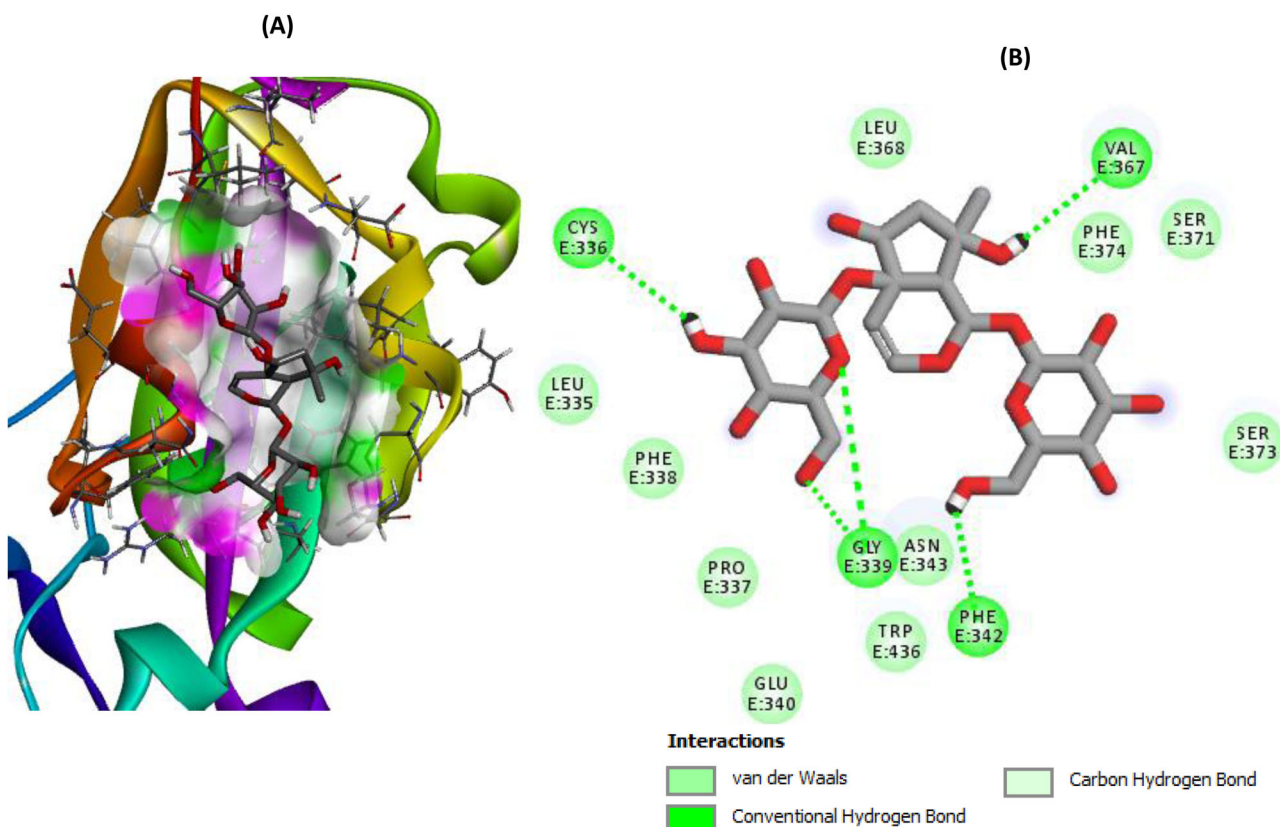


Figure 5. 3-D structure of (A) harpagide 5-O- β -D-glucopyranoside in complex with the ACE2 showing hydrogen bond donor-acceptor surface (B) 2-D representations displaying the interactions with amino acid residues.

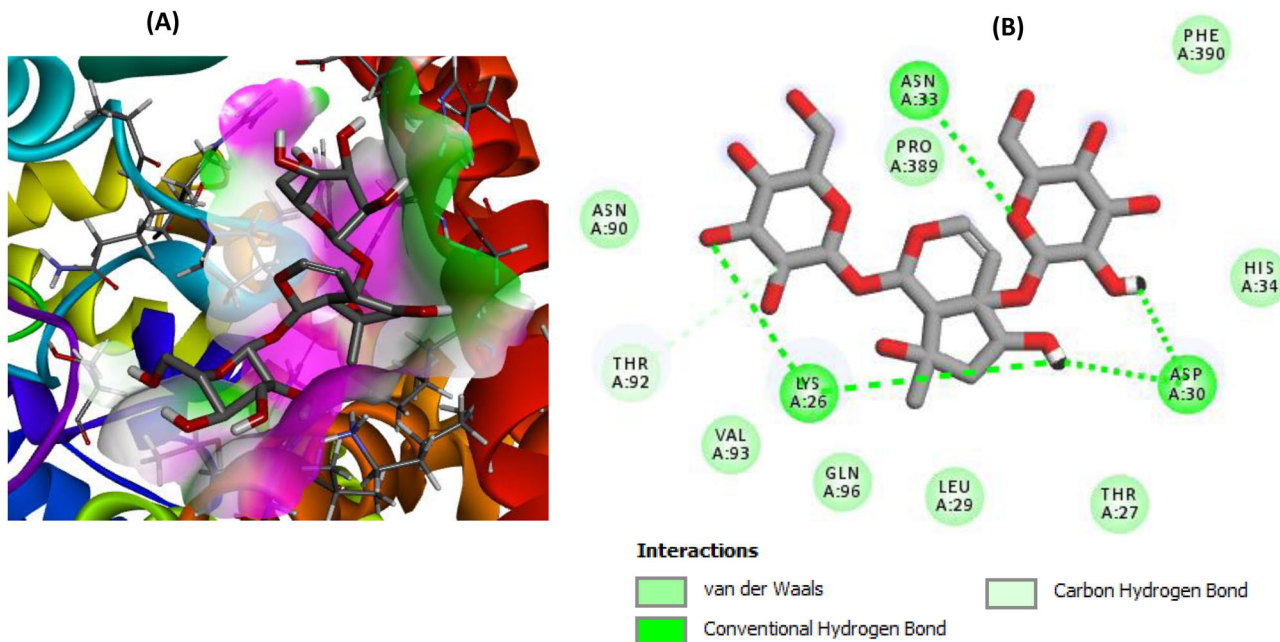


Figure 6. 3-D structure of (A) harpagide 5-O- β -D-glucopyranoside in complex with the Spike Protein showing hydrogen bond donor-acceptor surface (B) 2-D representations displaying the interactions with amino acid residues.

components of medicinal plants against COVID-19 is receiving a little or no attention at this time. This is without taking cognizance of the facts that even the so-called drugs (Chloroquine, Remdesivir, Azithromycin etc.) that are being repurposed against COVID-19 had traceable origin to

medicinal plants. Boosting the host immune system has also been reported to be beneficial in ameliorating the effect of the virus and the severe progression of the disease (Rothan & Byrareddy, 2020; Shi et al., 2020). In the present study, we investigated the epidemiology of COVID-19 and the

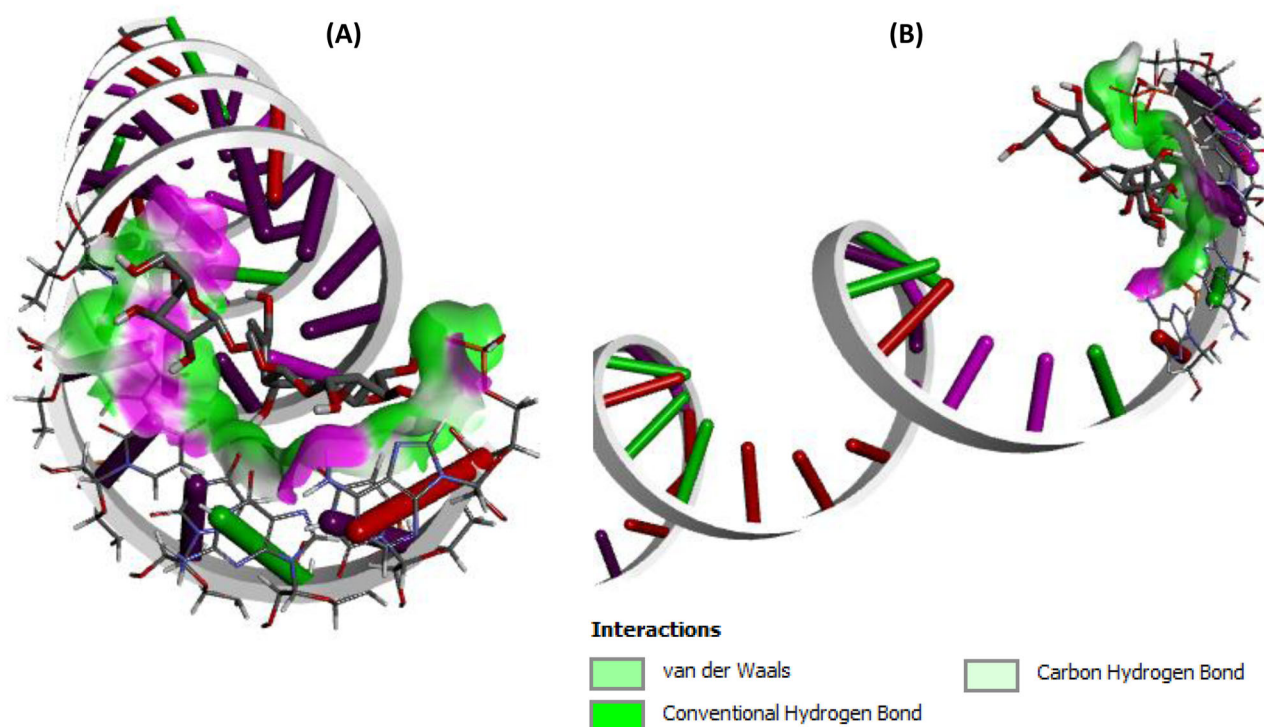


Figure 7. 3D structure of harpagide 5-O-β-D-glucopyranoside in complex with (A) translation initiation sequence (TIS); and (B) translation termination sequence (TTS).

Table 5. Binding energies of harpagide 5-O-β-D-glucopyranoside and standards drugs in kcal mol⁻¹.

Compounds	HG	AM	CQ	RV
Spike Protein	-7.7	-7.5	-5.9	-7.9
ACE2	-7.5	-6.2	-5.1	-5.7
Initiation Sequence	-6.4	-5.5	-3.7	-5.8
Termination Sequence	-6.3	-5.7	-4.3	-5.8

AM = Azithromycin, CQ = Chloroquine, RV = Remdesivir, ACE2: angiotensin converting enzyme 2 receptor spike protein binding domain, HG = harpagide 5-O-β-D-glucopyranoside.

potentials of harpagide 5-O-β-D-glucopyranoside, a new iridoid glycoside isolated from *C. volubile* leaves as a potential candidate for the inhibition of the proliferation of SARS-CoV-2.

The notable initial incidence and spatial distribution of COVID-19 cases and deaths across China (Figures 1A and 1B) can be attributed to its novelty (Guan et al., 2020; Sohrabi et al., 2020). This resulted in the disease being transmitted through hospitals and infected medical staff unknowingly. In addition, vulnerable cases, 60 years and above with underlying medical conditions such as diabetes, cardiovascular disease, hypertension, asthma and other respiratory diseases contributed to the majority of the cases and deaths in China (Zhang, 2020). However, the downward trend of the disease in China (Figures 1C – 1F) can be related to her timely amendment of governmental policies which included enforcing restricted personnel movements in the epicentre of the disease (Wuhan city) and other areas of China (Gan et al., 2020; Kraemer et al., 2020; Zhu et al., 2020), sharing vital prevention and control information (including wearing of masks, adequate washing and sanitizing of hands, symptoms and means of seek medical assistance), enhanced public health resources, providing improved and functional infectious

disease surveillance, early detection systems and multi-sectoral rapid response systems to assist curtail the disease (Zhang, 2020). China's overall initiative and strategies in response to COVID-19 can be attributed to the lessons and experiences of the SARS epidemic that occurred in 2003 (Zhang, 2020). Contrarily, limited medical resources and the delayed response in implementing policies restricting movements of people may have resulted in the surge of cases and deaths across Europe and other countries with high confirmed cases and deaths (Figures 1E and 1F). In other words, countries reacted slowly in implementing measures and policies to reduce the chance of contact between infected and vulnerable people. While the low recorded COVID-19 cases and related deaths across Africa can be linked with few vulnerable populations because Africa's life expectancy at birth is 61 years (World Health Organisation, 2018). Thus, a global health emergency that involves continuous collaborative surveillance, information sharing, researching and implementing evidence-based public health and clinical practices and formulating effective control strategies cannot be overemphasised. Furthermore, in-depth studies aimed at assessing the vulnerability of young people with underlying medical conditions and amongst different blood groups is important. These measures would be instrumental in the implementation of targeted intervention policies and resources.

The ¹H NMR spectral of the isolated compound was compared to that of harpagide and allobentonoside, compounds of close structural similarity as obtained in literatures (Jensen et al., 1989; Manguro et al., 2011; Venditti et al., 2017). While harpagide has only one glucose unit attached at C-1 to the iridoid aglycone unit, the allobentonoside has two glucose units attached at C-1 and C-5 as in harpagide 5-

O- β -D-glucopyranoside. However, allobentonicoside has the hydroxyl converted to a carbonyl at C-6 with an unsaturation at C-7. The isolated compound has very similar ^1H and ^{13}C NMR data compared to the allobentonicoside (Figure S1). However, the absence of carbonyl stretching vibration in the infrared spectrum confirms that the compound is not allobentonicoside. The molecular ion peak at m/z 549 obtained from FAB-MS for the isolated compound which corresponds to $\text{C}_{21}\text{H}_{34}\text{O}_{15}$ $[\text{M} + \text{Na}]$ further strengthens the claim of two attached glucose units as in allobentonicoside. The de-glucosidated aglycone was presented at m/z 387 calculated for $\text{C}_{15}\text{H}_{26}\text{O}_{10}$ in the FAB-MS spectrum. The isolated compound was thus presented as harpagide 5-O- β -D-glucopyranoside as depicted in Figure 2.

The DFT calculated result for the ^1H -NMR and the calculated vibrational frequencies obtained showed good agreement with experimental (Figure 3). The ^1H -NMR chemical shifts, with a small deviation of 0.01 and 0.11 ppm for H-4 and H-9 (Table 2), respectively. Others displayed slightly increased deviations from the experimental values, though these deviations are in accordance with previously calculated DFT ^1H -NMR calculations (De Souza et al., 2017; Olanrewaju et al., 2020).

Druglikeness properties of compounds screen-out promising ligands that are likely to be used as drugs based on some identified properties (Dong et al., 2018). The properties comprise those considered crucial for both kinetic and dynamic interactions inside the biological system. Essentially, harpagide 5-O- β -D-glucopyranoside displayed a potential druggable character, with the exception of a very few properties (Table 3). Molecular weight indicates the mass as well as the size of a ligand and plays a greater role in determining the solubility, absorption and distribution of a given drug candidate (Doak et al., 2014). Basically, the molecular weight of the new ligands reported in this work appears to fit within the acceptable range of this parameter. Hydrogen bond acceptors and donors in drug structures play an important role in water solubility, membrane transport, distribution, and drug-receptor interactions (Cheng et al., 2007; Kumar et al., 2010). Five hydrogen bond donors and ten hydrogen bond acceptors are required for a ligand to possess a satisfactory bioavailability and the optimum number of drug-target interactions via hydrogen bonds (Dong et al., 2018). LogP indicates a relative concentration of the solute in octanol and water (octanol-water partition coefficient). It determines the degree of hydrophobicity of a ligand and plays a role in predicting drug absorption via the phospholipid bilayer of the cell membrane (Kumar et al., 2010). Generally, a more polar compound typically encounters difficulties when passing through phospholipid bilayer of the cell membrane (Yusof & Segall, 2013). Harpagide 5-O- β -D-glucopyranoside demonstrated approvingly a very good partition coefficient (Table 3). This suggests that it can be efficiently transported across cell membranes, as passive diffusion through a cell membrane is a key element of transcellular absorption (Doak et al., 2014; Yusof et al., 2014).

The isolated compound was subjected to *in silico* pharmacokinetics and lethal toxicity analysis in order to predict its

possible drug-drug interactions and toxicity when swallowed (Table 4). The low GI absorption value insinuates harpagide 5-O- β -D-glucopyranoside may not be easily absorbed by the intestine. The small intestine is known for its important role in drug metabolism as the large surfaces areas of villi and microvilli determine the rate of drug absorption via the oral route (Pang, 2003). The low absorption of the compound may be attributed to its inability to permeate the phospholipid bilayers of the intestinal membrane owing to the lipophobic properties of most glycosides (Chao et al., 2006). This may also be responsible for the predicted impermeability of the compound across the BBB. The prediction of the compound as a substrate of P-gp, suggests it is translocated from the intracellular to the extracellular compartment via transmembrane efflux mediated by P-gp (Kim, 2002). This may be responsible for the low GI absorption of the compound as P-gp has been implicated in reduced bioavailability of its substrate (Constantinides & Wasan, 2007). The predicted inability of the compound to inhibit CYPs 1A2, 2C19, 2C9, 2D6 and 3A4 insinuates that there will be little or no drug – drug interactions when co-administered with other drugs which are metabolized by these enzymes (Obach et al., 2006). The predicted LD_{50} value of 2000 mg/kg and toxicity class of 4 suggest the compound is safe for administration (Banerjee et al., 2018).

Phagocytic respiratory oxidative burst has been implicated in innate immunity and inflammatory processes which are the major pathogenesis of COVID-19. Boosting the immune system particularly during the incubation and non-severe stages of the disease, has been recognized as a strategy to eliminate the virus and to suppress the progression to severe stages (Shi et al., 2020). Phagocytic respiratory oxidative burst involves the generation of ROS from increased non – mitochondrial oxygen consumption arising from dehydrogenation of glucose via the hexose monophosphate shunt (Allen, 1994; Erukainure, Hafizur, et al., 2017). Continuous phagocytic-induced ROS production will lead to an imbalance in the innate antioxidant system, thereby resulting in oxidative stress and provocation of inflammatory cytokines (Ciz et al., 2012). Exacerbated inflammatory cytokine production often regarded as cytokine release syndrome (CRS) has been implicated in the onset and progression of COVID-19 stages (Mehta et al., 2020; Shi et al., 2020). Thus, arresting phagocytic respiratory oxidative bursts may be a therapeutic strategy in treating and managing the disease and its progression. In the present study, harpagide 5-O- β -D-glucopyranoside suppressed the production of ROS in PMNs as shown in Figure 4A. Thus, indicating a suppressive activity on phagocytic respiratory oxidative burst and may be a good drug candidate in the treatment and management of COVID-19 and its complications. This activity correlates with our previous reports on the ability of extracts and isolated compounds from *C. voluble* leaves and flower to modulate phagocytic oxidative burst in whole blood, PMNs and macrophages (Erukainure, Hafizur, et al., 2017; Erukainure, Mesaik, et al., 2017; Erukainure et al., 2016).

The suppressive activity on respiratory oxidative burst by harpagide 5-O- β -D-glucopyranoside is further corroborated

by its ability to suppress T-cell proliferation (Figure 4B). Proliferation of T-cell has been implicated in the activation of CRS, and studies have suggested that targeting T-cell proliferation may suppress the severe progression of COVID-19 (Zhou et al., 2020).

At molecular level, the viral envelope spike (S) protein of SARS-CoV-2 and angiotensin converting enzyme 2 receptor within the host are central to COVID-19 pathogenesis and response to therapeutic interventions among other biological factors (Tian et al., 2020). Basically, it has been reported that envelope spike (S) protein is important for coronavirus pathogenesis as it mediates receptor binding and membrane fusion implicated in host tropism and transmission capability (He et al., 2020). Mostly, the S protein is functionally divided into the S1 domain, responsible for receptor binding, and S2 domain, responsible for cell membrane fusion. Structure analysis suggests that the receptor-binding domain is composed of a core and an external subdomain. Angiotensin converting enzyme 2 (ACE2) has been reported to act as a cell receptor for the S protein (Kuster et al., 2020). Therefore, targeting S protein and ACE2 at transcriptomic and proteomic levels could be a novel strategy for treatment and management of COVID-19. The docking simulations revealed that harpagide 5-O- β -D-glucopyranoside binds better with the evidence of hydrogen bonding interactions with amino acid residues around the binding pocket of the host receptor target as well as the nitrogenous base and ribose sugar of the mRNA sequence of initiation and termination sequence of the viral spike protein mRNA (Figures 5–7). Remdesivir in complex with SARS-CoV-2 spike protein displayed stronger molecular interactions when compared with CQ and AM (Figure S3). However, it is comparable with harpagide 5-O- β -D-glucopyranoside. This can be as a result of the four hydrogen bonding interactions with four amino acid residues in the bind pocket of the SARS-CoV-2 spike protein compared to three of hydrogen bonding interactions found in harpagide 5-O- β -D-glucopyranoside (Figure S2). Remdesivir have been reported the recently to inhibit novel SARS-CoV-2 *in vitro*, which invariably corroborated our findings (Table 5) (Wang et al., 2020). The good binding potential of Harpagide 5-O- β -D-glucopyranoside can prevent or impair the recruitment of initiating and termination factors around mRNA sequence, thus affecting the ultimate translation of S protein mRNA. Equally, the strong and robust interactions were visible between the compound and S protein as well as ACE2 receptor (Figures 6 and 7). Thus, qualifying it as a potential inhibitor of S protein mRNA translation vis-à-vis barriers that affect S protein and ACE2 receptor interactions implicated in COVID-19 pathogenesis (Kuster et al., 2020). However, further studies are needed to evaluate the actual efficacy of HG against SARS-CoV-2 at *in vitro* and *in vivo* levels while targeting spike protein and its receptor at transcriptomic and proteomic levels.

Conclusion

Taken together, these results suggest the immunomodulatory properties of harpagide 5-O- β -D-glucopyranoside isolated from *C. volubile* leaves which may be explored in the

treatment and management of COVID-19. This is further corroborated by its strong molecular interaction and binding with the translation initiation and termination sequence sites of S protein mRNA and S protein of SARS-COV-2 and its host receptor protein (ACE2 receptor). In addition, there is a need for implementation of targeted intervention policies and resources which should include a global health emergency involving continuous collaborative surveillance, information sharing, research and implementation of evidence-based public health and clinical practices.

Acknowledgements

OE acknowledges The World Academy of Science (TWAS) for 2012 ICCBS-TWAS fellowship at the H.E.J. Research Institute of Chemistry, ICCBS, University of Karachi, Karachi, Pakistan.

Disclosure statement

No potential conflict of interest was reported by the authors.

Funding

This work was supported by The World Academy of Sciences.

ORCID

Ochuko L. Erukainure  <http://orcid.org/0000-0003-0489-338X>
Olubunmi Atolani  <http://orcid.org/0000-0002-3580-5904>
Aliyu Muhammad  <http://orcid.org/0000-0002-4167-7793>

References

- Allen, R. C. (1994). Role of oxygen in phagocyte microbicidal action. *Environmental Health Perspectives*, 102(suppl 10), 201–208.
- Alyiu, M., Odunola, O. A., Farooq, A. D., Mesaik, A. M., Choudhary, M. I., Azhar, M., Asif, M. M., & Erukainure, O. L. (2014). Antioxidant, mitogenic and immunomodulatory potentials of acacia honey. *Nutritional Therapy & Metabolism*, 32(2), 68–78. doi: 10.5301/NTM.2014.12285
- Banerjee, P., Eckert, A. O., Schrey, A. K., & Preissner, R. (2018). ProTox-II: A webserver for the prediction of toxicity of chemicals. *Nucleic Acids Research*, 46(W1), W257–W263. <https://doi.org/10.1093/nar/gky318>
- Burkill, H. M. (1985). *The useful plants of west tropical Africa*. (2nd ed., Vol. 1). Kew, Royal Botanic Gardens.
- Cances, E., Mennucci, B., & Tomasi, J. (1997). A new integral equation formalism for the polarizable continuum model: Theoretical background and applications to isotropic and anisotropic dielectrics. *The Journal of Chemical Physics*, 107(8), 3032–3041.
- Chao, P.-D L., Hsiu, S.-L., & Hou, Y.-C. (2006). Bioavailability, metabolism, and pharmacokinetics of glycosides in Chinese herbs. In M. Wang, S. Sang, L. S. Hwang, & C.-T. Ho (Eds.), *Herbs: Challenges in chemistry and biology* (pp. 212–223). ACS Publications.
- Cheng, A. C., Coleman, R. G., Smyth, K. T., Cao, Q., Soulard, P., Caffrey, D. R., Salzberg, A. C., & Huang, E. S. (2007). Structure-based maximal affinity model predicts small-molecule druggability. *Nature Biotechnology*, 25(1), 71–75. <https://doi.org/10.1038/nbt1273>
- Ciz, M., Denev, P., Kratchanova, M., Vasicek, O., Ambrozova, G., & Lojek, A. (2012). Flavonoids inhibit the respiratory burst of neutrophils in mammals. *Oxidative Medicine and Cellular Longevity*, 2012, 181295. doi: 10.1155/2012/181295
- Constantinides, P. P., & Wasan, K. M. (2007). Lipid formulation strategies for enhancing intestinal transport and absorption of P-glycoprotein (P-gp) substrate drugs: In vitro/in vivo case studies. *Journal of*

- Pharmaceutical Sciences*, 96(2), 235–248. <https://doi.org/10.1002/jps.20780>
- da Silva, R. G., Ribeiro, M. H. D. M., Mariani, V. C., & dos Santos Coelho, L. (2020). Forecasting Brazilian and American COVID-19 cases based on artificial intelligence coupled with climatic exogenous variables. *Chaos, Solitons, and Fractals*, 139, 110027. <https://doi.org/10.1016/j.chaos.2020.110027>
- Daina, A., Michielin, O., & Zoete, V. (2017). SwissADME: A free web tool to evaluate pharmacokinetics, drug-likeness and medicinal chemistry friendliness of small molecules. *Scientific Reports*, 7, 42717. <https://doi.org/10.1038/srep42717>
- De Souza, L. A., Tavares, W. M., Lopes, A. P. M., Soeiro, M. M., & De Almeida, W. B. (2017). Structural analysis of flavonoids in solution through DFT 1H NMR chemical shift calculations: Epigallocatechin, Kaempferol and Quercetin. *Chemical Physics Letters*, 676, 46–52.
- Doak, B. C., Over, B., Giordanetto, F., & Kihlberg, J. (2014). Oral druggable space beyond the rule of 5: Insights from drugs and clinical candidates. *Chemistry & Biology*, 21(9), 1115–1142. <https://doi.org/10.1016/j.chembiol.2014.08.013>
- Dong, J., Wang, N.-N., Yao, Z.-J., Zhang, L., Cheng, Y., Ouyang, D., Lu, A.-P., & Cao, D.-S. (2018). ADMETlab: A platform for systematic ADMET evaluation based on a comprehensively collected ADMET database. *Journal of Cheminformatics*, 10(1), 29. doi: 10.1186/s13321-018-0283-x
- Erukainure, O. L., Ashraf, N., Naqvi, A. S., Zaruwa, M. Z., Muhammad, A., Odusote, A. D., & Elemo, G. N. (2018). Fatty acids rich extract from clerodendrum volubile suppresses cell migration; abates oxidative stress; and regulates cell cycle progression in glioblastoma multiforme (U87 MG) cells. *Frontiers in Pharmacology*, 9, 251. <https://doi.org/10.3389/fphar.2018.00251>
- Erukainure, O. L., Hafizur, R. M., Choudhary, M. I., Adhikari, A., Mesaik, A. M., Atolani, O., Banerjee, P., Preissner, R., Muhammad, A., & Islam, M. S. (2017). Anti-diabetic effect of the ethyl acetate fraction of *Clerodendrum volubile*: Protocatechuic acid suppresses phagocytic oxidative burst and modulates inflammatory cytokines. *Biomedicine & Pharmacotherapy*, 86, 307–315.
- Erukainure, O. L., Hafizur, R. M., Kabir, N., Choudhary, M. I., Atolani, O., Banerjee, P., Preissner, R., Chukwuma, C. I., Muhammad, A., Amonsou, E. O., & Islam, M. S. (2018). Suppressive effects of clerodendrum volubile P Beauv. [Labiatae] methanolic extract and its fractions on type 2 diabetes and its complications. *Frontiers in Pharmacology*, 9, 8. doi: 10.3389/fphar.2018.00008
- Erukainure, O. L., Ijomone, O. M., Chukwuma, C. I., Xiao, X., Salau, V. F., & Islam, M. S. (2020). *Dacryodes edulis* (G. Don) HJ Lam modulates glucose metabolism, cholinergic activities and Nrf2 expression, while suppressing oxidative stress and dyslipidemia in diabetic rats. *Journal of Ethnopharmacology*, 255, 112744.
- Erukainure, O. L., Mesaik, M. A., Atolani, O., Muhammad, A., Chukwuma, C. I., & Islam, M. S. (2017). Pectolarigenin from the leaves of *Clerodendrum volubile* shows potent immunomodulatory activity by inhibiting T – cell proliferation and modulating respiratory oxidative burst in phagocytes. *Biomedicine & Pharmacotherapy*, 93, 529–535.
- Erukainure, O. L., Mesaik, A. M., Muhammad, A., Chukwuma, C. I., Manhas, N., Singh, P., Aremu, O. S., & Islam, M. S. (2016). Flowers of *Clerodendrum volubile* exacerbate immunomodulation by suppressing phagocytic oxidative burst and modulation of COX-2 activity. *Biomedicine & Pharmacotherapy*, 83, 1478–1484.
- Erukainure, O. L., Narainpersad, N., Singh, M., Olakunle, S., & Islam, M. S. (2018). *Clerodendrum volubile* inhibits key enzymes linked to type 2 diabetes but induces cytotoxicity in human embryonic kidney (HEK293) cells via exacerbated oxidative stress and proinflammation. *Biomedicine & Pharmacotherapy*, 106, 1144–1152.
- Erukainure, O., Oke, O., Ajiboye, A., & Okafor, O. (2011). Nutritional qualities and phytochemical constituents of *Clerodendrum volubile*, a tropical non-conventional vegetable. *International Food Research Journal*, 18(4), 1393–1399.
- Erukainure, O. L., Sanni, O., & Islam, M. S. (2018). *Clerodendrum volubile*: Phenolics and applications to health. In R. Watson, V. Preedy, & S. Zibadi (Eds.), *Polyphenols: Mechanisms of action in human health and disease* (2nd ed.). Elsevier.
- Erukainure, O. L., Zaruwa, M. Z., Mesaik, A. M., Muhammad, A., Adoga, J. O., Ogunyemi, I. O., Ebuehi, O. A. T., & Elemo, G. N. (2017). Suppression of phagocytic oxidative burst, cytotoxic effect, and computational prediction of oral toxicity of dietary fatty acids of *Clerodendrum volubile* stem. *Comparative Clinical Pathology*, 26(3), 663–671.
- European Centre for Disease Prevention and Control (ECDC). (2020). COVID-19 data. Retrieved September 02, 2020, from, <https://www.ecdc.europa.eu/en/covid-19-pandemic>
- Frisch, M., Trucks, G., Schlegel, H. B., Scuseria, G., Robb, M., Cheeseman, J. R., Scalmani, G., Barone, V., Mennucci, B., & Petersson, G. (2009). *Gaussian 09, revision D. 01*. Gaussian, Inc.
- Gan, H., Zhang, Y., Yuan, M., Wu, X., Liu, Z., Liu, M., Wu, J., Xu, S., Gong, L., Xu, H., & Tao, F. (2020). Epidemiological characteristics of 1 052 cases of COVID-19 in epidemic clusters. *Chinese Journal of Epidemiology*, 41(5), E027. <https://doi.org/10.3760/cma.j.cn112338-20200301-00223>
- Guan, W.-J., Ni, Z.-Y., Hu, Y., Liang, W.-H., Ou, C.-Q., He, J.-X., Liu, L., Shan, H., Lei, C.-L., Hui, D. S. C., Du, B., Li, L.-J., Zeng, G., Yuen, K.-Y., Chen, R.-C., Tang, C.-L., Wang, T., Chen, P.-Y., Xiang, J., ... Zhong, N.-S. (2020). Clinical characteristics of coronavirus disease 2019 in China. *New England Journal of Medicine*, 382(18), 1708–1720.
- Guo, Y.-R., Cao, Q.-D., Hong, Z.-S., Tan, Y.-Y., Chen, S.-D., Jin, H.-J., Tan, K.-S., Wang, D.-Y., & Yan, Y. (2020). The origin, transmission and clinical therapies on coronavirus disease 2019 (COVID-19) outbreak—an update on the status. *Military Medical Research*, 7(1), 1–10.
- Gurwitz, D. (2020). Angiotensin receptor blockers as tentative SARS-CoV-2 therapeutics. *Drug Development Research*, 81(5), 537–540. doi: 10.1002/ddr.21656
- Harun, N. H., Septama, A. W., & Jantan, I. (2015). Immunomodulatory effects of selected Malaysian plants on the CD18/11a expression and phagocytosis activities of leukocytes. *Asian Pacific Journal of Tropical Biomedicine*, 5(1), 48–53.
- He, F., Deng, Y., & Li, W. (2020). Coronavirus disease 2019: What we know? *Journal of Medical Virology*, 92(7), 719–725. <https://doi.org/10.1002/jmv.25766>
- Helfand, S. L., Werkmeister, J., & Roder, J. C. (1982). Chemiluminescence response of human natural killer cells. I. The relationship between target cell binding, chemiluminescence, and cytolysis. *The Journal of Experimental Medicine*, 156(2), 492–505. <https://doi.org/10.1084/jem.156.2.492>
- Holman, N., Knighton, P., Kar, P., O’Keefe, J., Curley, M., Weaver, A., Barron, E., Bakhai, C., Khunti, K., & Wareham, N. J. (2020). Risk factors for COVID-19-related mortality in people with type 1 and type 2 diabetes in England: A population-based cohort study. *The Lancet Diabetes & Endocrinology*, 8(10), 823–833.
- Jayaram, B., Singh, T., Mukherjee, G., Mathur, A., Shekhar, S., & Shekhar, V. (2012). Sanjeevini: A freely accessible web-server for target directed lead molecule discovery. *BMC Bioinformatics*, 13(S17), S7. <https://doi.org/10.1186/1471-2105-13-S17-S7>
- Jensen, S. R., Nielsen, B. J., & Rickelt, L. F. (1989). Iridoids in *Physostegia virginiana*. *Phytochemistry*, 28(11), 3055–3057.
- Jiang, S., Lu, L., Liu, Q., Xu, W., & Du, L. (2012). Receptor-binding domains of spike proteins of emerging or re-emerging viruses as targets for development of antiviral vaccines. *Emerging Microbes & Infections*, 1(1), 1–8. doi: 10.1038/emi.2012.1
- Johnson, R. D. III, (1999). *NIST 101. Computational chemistry comparison and benchmark database*. <http://srdata.nist.gov/cccbdb/>
- Kim, R. B. (2002). Drugs as P-glycoprotein substrates, inhibitors, and inducers. *Drug Metabolism Reviews*, 34(1–2), 47–54. <https://doi.org/10.1081/dmr-120001389>
- Kraemer, M. U. G., Yang, C.-H., Gutierrez, B., Wu, C.-H., Klein, B., Pigott, D. M., Du Plessis, L., Faria, N. R., Li, R., Hanage, W. P., Brownstein, J. S., Layan, M., Vespignani, A., Tian, H., Dye, C., Pybus, O. G., & Scarpino, S. V. (2020). The effect of human mobility and control measures on the COVID-19 epidemic in China. *Science (New York, N.Y.)*, 368(6490), 493–497. <https://doi.org/10.1126/science.abb4218>
- Kumar, B. P., Soni, M., Bhikhalal, U. B., Kakkot, I. R., Jagadeesh, M., Bommu, P., & Nanjan, M. (2010). Analysis of physicochemical

- properties for drugs from nature. *Medicinal Chemistry Research*, 19(8), 984–992.
- Kuster, G. M., Pfister, O., Burkard, T., Zhou, Q., Twerenbold, R., Haaf, P., Widmer, A. F., & Osswald, S. (2020). SARS-CoV2: Should inhibitors of the renin-angiotensin system be withdrawn in patients with COVID-19? *European Heart Journal*, 41(19), 1801–1803. <https://doi.org/10.1093/eurheartj/ehaa235>
- Lan, J., Ge, J., Yu, J., Shan, S., Zhou, H., Fan, S., Zhang, Q., Shi, X., Wang, Q., Zhang, L., & Wang, X. (2020). Structure of the SARS-CoV-2 spike receptor-binding domain bound to the ACE2 receptor. *Nature*, 581(7807), 215–220. <https://doi.org/10.1038/s41586-020-2180-5>
- Lipinski, C. A. (2004). Lead- and drug-like compounds: The rule-of-five revolution. *Drug Discovery Today. Technologies*, 1(4), 337–341. <https://doi.org/10.1016/j.ddtec.2004.11.007>
- Manguro, L. O. A., Lemmen, P., & Hao, P. (2011). Iridoid glycosides from underground parts of *Ajuga remota*. *Records of Natural Products*, 5(3), 147–157.
- Mehta, P., McAuley, D. F., Brown, M., Sanchez, E., Tattersall, R. S., & Manson, J. J. (2020). COVID-19: Consider cytokine storm syndromes and immunosuppression. *The Lancet*, 395(10229), 1033–1034. doi: 10.1016/S0140-6736(20)30630-9
- Mitjà, O., & Clotet, B. (2020). Use of antiviral drugs to reduce COVID-19 transmission. *The Lancet. Global Health*, 8(5), e639–e640. doi: 10.1016/S2214-109X(20)30114-5
- Morris, G. M., Huey, R., Lindstrom, W., Sanner, M. F., Belew, R. K., Goodsell, D. S., & Olson, A. J. (2009). AutoDock4 and AutoDockTools4: Automated docking with selective receptor flexibility. *Journal of Computational Chemistry*, 30(16), 2785–2791. <https://doi.org/10.1002/jcc.21256>
- Nielsen, M., Lundegaard, C., Worning, P., Lauemøller, S. L., Lamberth, K., Buus, S., Brunak, S., & Lund, O. (2003). Reliable prediction of T-cell epitopes using neural networks with novel sequence representations. *Protein Science : A Publication of the Protein Society*, 12(5), 1007–1017. <https://doi.org/10.1110/ps.0239403>
- Obach, R. S., Walsky, R. L., Venkatakrishnan, K., Gaman, E. A., Houston, J. B., & Tremaine, L. M. (2006). The utility of in vitro cytochrome P450 inhibition data in the prediction of drug-drug interactions. *The Journal of Pharmacology and Experimental Therapeutics*, 316(1), 336–348. <https://doi.org/10.1124/jpet.105.093229>
- Oboh, G., Ogunruku, O. O., Oyeleye, S. I., Olasehinde, T. A., Ademosun, A. O., & Boligon, A. A. (2017). Phenolic extracts from *Clerodendrum volubile* leaves inhibit cholinergic and monoaminergic enzymes relevant to the management of some neurodegenerative diseases. *Journal of Dietary Supplements*, 14(3), 358–371.
- Olanrewaju, A. A., Fabiyi, F. S., Ibeji, C. U., Kolawole, E. G., & Gupta, R. (2020). Synthesis, spectral, structure and computational studies of novel transition Metal (II) complexes of (Z)-((dimethylcarbamothioyl)thio)((1, 1, 1-trifluoro-4-(naphthalen-2-yl)-4-oxobut-2-en-2-yl)oxy). *Journal of Molecular Structure*, 1211, 128057.
- Onder, G., Rezza, G., & Brusaferro, S. (2020). Case-fatality rate and characteristics of patients dying in relation to COVID-19 in Italy. *JAMA*, 323(18), 1775–1776. <https://doi.org/10.1001/jama.2020.4683>
- Pang, K. S. (2003). Modeling of intestinal drug absorption: Roles of transporters and metabolic enzymes (for the Gillette Review Series). *Drug Metabolism and Disposition: The Biological Fate of Chemicals*, 31(12), 1507–1519. <https://doi.org/10.1124/dmd.31.12.1507>
- Pascarella, G., Strumia, A., Pilliego, C., Bruno, F., Del Buono, R., Costa, F., Scarlata, S., & Agrò, F. E. (2020). COVID-19 diagnosis and management: A comprehensive review. *Journal of Internal Medicine*, 288(2), 192–206. <https://doi.org/10.1111/joim.13091>
- Rothan, H. A., & Byrareddy, S. N. (2020). The epidemiology and pathogenesis of coronavirus disease (COVID-19) outbreak. *Journal of Autoimmunity*, 109, 102433. <https://doi.org/10.1016/j.jaut.2020.102433>
- Roser, M., Ritchie, H., Ortiz-Ospina, E., & Hasell, J. (2020). Coronavirus Pandemic (COVID-19). Our World In Data 2020. Retrieved September 02, 2020, from, '<https://ourworldindata.org/coronavirus>' [Online Resource].
- Sanner, M. F. (1999). Python: A programming language for software integration and development. *Journal of Molecular Graphics & Modelling*, 17(1), 57–61.
- Schoeman, D., & Fielding, B. C. (2019). Coronavirus envelope protein: Current knowledge. *Virology Journal*, 16(1), 69. <https://doi.org/10.1186/s12985-019-1182-0>
- Shi, Y., Wang, Y., Shao, C., Huang, J., Gan, J., Huang, X., Bucci, E., Piacentini, M., Ippolito, G., & Melino, G. (2020). COVID-19 infection: The perspectives on immune responses. *Cell Death Differ*, 27(5), 1451–1454. <https://doi.org/10.1038/s41418-020-0530-3>
- Sohrabi, C., Alsafi, Z., O'Neill, N., Khan, M., Kerwan, A., Al-Jabir, A., Iosifidis, C., & Agha, R. (2020). World Health Organization declares global emergency: A review of the 2019 novel coronavirus (COVID-19). *International Journal of Surgery (London, England)*, 76, 71–76. <https://doi.org/10.1016/j.ijsu.2020.02.034>
- Tang, D., Li, J., Zhang, R., Kang, R., & Klionsky, D. J. (2020). Chloroquine in fighting COVID-19: Good, bad, or both? *Autophagy*, doi: 10.1080/15548627.2020.1796014
- Thamkaew, G., Sjöholm, I., & Galindo, F. G. (2020). A review of drying methods for improving the quality of dried herbs. *Critical Reviews in Food Science and Nutrition*. doi:10.1080/10408398.2020.1765309
- Tian, X., Li, C., Huang, A., Xia, S., Lu, S., Shi, Z., Lu, L., Jiang, S., Yang, Z., Wu, Y., & Ying, T. (2020). Potent binding of 2019 novel coronavirus spike protein by a SARS coronavirus-specific human monoclonal antibody. *Emerging Microbes & Infections*, 9(1), 382–385. <https://doi.org/10.1080/22221751.2020.1729069>
- Truong, D.-H., Nguyen, D. H., Ta, N. T. A., Bui, A. V., Do, T. H., & Nguyen, H. C. (2019). Evaluation of the use of different solvents for phytochemical constituents, antioxidants, and in vitro anti-inflammatory activities of *Severinia buxifolia*. *Journal of Food Quality*, 2019, 1–9. doi: 10.1155/2019/8178294
- Venditti, A., Frezza, C., Lorenzetti, L. M., Maggi, F., Serafini, M., & Bianco, A. (2017). Reassessment of the polar fraction of *Stachys alopecuroides* (L.) Benth. subsp. *divulsa* (Ten.) Grande (Lamiaceae) from the Monti Sibillini National Park: A potential source of bioactive compounds. *Journal of Intercultural Ethnopharmacology*, 6(2), 144–153. <https://doi.org/10.5455/jice.20170327073801>
- Vijayan, P., Raghu, C., Ashok, G., Dhanaraj, S., & Suresh, B. (2004). Antiviral activity of medicinal plants of Nilgiris. *The Indian Journal of Medical Research*, 120(1), 24–29.
- Wang, M., Cao, R., Zhang, L., Yang, X., Liu, J., Xu, M., Shi, Z., Hu, Z., Zhong, W., & Xiao, G. (2020). Remdesivir and chloroquine effectively inhibit the recently emerged novel coronavirus (2019-nCoV) in vitro. *Cell Research*, 30(3), 269–271. <https://doi.org/10.1038/s41422-020-0282-0>
- Wang, Y., Zhang, D., Du, G., Du, R., Zhao, J., Jin, Y., Fu, S., Gao, L., Cheng, Z., Lu, Q., Hu, Y., Luo, G., Wang, K., Lu, Y., Li, H., Wang, S., Ruan, S., Yang, C., Mei, C., et al. (2020). Remdesivir in adults with severe COVID-19: A randomised, double-blind, placebo-controlled, multicenter trial. *The Lancet*, 395(10236), 1569–1578.
- WHO. (2020, April 1). *Coronavirus disease 2019 (COVID-19): Situation report*, 67. <https://apps.who.int/iris/bitstream/handle/10665/331613/nCoVsitrep27Mar2020-eng.pdf> on
- Wolinski, K., Hinton, J. F., & Pulay, P. (1990). Efficient implementation of the gauge-independent atomic orbital method for NMR chemical shift calculations. *Journal of the American Chemical Society*, 112(23), 8251–8260.
- World Health Organisation. (2018). *Mortality and burden of disease*. <https://data.worldbank.org/indicator/SP.DYN.LE00.IN?locations=ZG>
- Yang, B., Hao, F., Li, J., Chen, D., & Liu, R. (2013). Binding of chrysoidine to catalase: Spectroscopy, isothermal titration calorimetry and molecular docking studies. *Journal of Photochemistry and Photobiology. B, Biology*, 128, 35–42. <https://doi.org/10.1016/j.jphoto-biol.2013.08.006>
- Yusof, I., & Segall, M. D. (2013). Considering the impact drug-like properties have on the chance of success. *Drug Discovery Today*, 18(13–14), 659–666. <https://doi.org/10.1016/j.drudis.2013.02.008>
- Yusof, I., Shah, F., Hashimoto, T., Segall, M. D., & Greene, N. (2014). Finding the rules for successful drug optimisation. *Drug*

- Discovery Today*, 19(5), 680–687. <https://doi.org/10.1016/j.drudis.2014.01.005>
- Zhang, Y. (2020). Analysis of Epidemiological characteristics of new coronavirus pneumonia. *Chinese Journal of Epidemiology*, 41(2), 1–7.
- Zhou, D., Dai, S.-M., & Tong, Q. (2020). COVID-19: A recommendation to examine the effect of hydroxychloroquine in preventing infection and progression. *The Journal of Antimicrobial Chemotherapy*, 75(7), 1667–1670. <https://doi.org/10.1093/jac/dkaa114>
- Zhou, Y., Hou, Y., Shen, J., Huang, Y., Martin, W., & Cheng, F. (2020). Network-based drug repurposing for novel coronavirus 2019-nCoV/SARS-CoV-2. *Cell Discovery*, 6(1), 14–18.
- Zhu, Z., Zhong, C., Zhang, K., Dong, C., Peng, H., Xu, T., Wang, A. L., Guo, Z. R., Zhang, Y. (2020). Epidemic trend of corona virus disease 2019 (COVID-19) in mainland China. *Chinese Journal of Preventive Medicine*, 54, E022–E022. <https://doi.org/10.3760/cma.j.cn112150-20200222-00163>